**Mohammed Wadi[1,*],
Wisam Elmasry[2],**

Regular paper

Comparison of Five Different Distributions based on Three Metaheuristics to Model Wind Speed Distribution

Wind energy Modelling is crucial in studying any site s feasibility. Wind energy Modelling principally depends on wind speed distribution. Determining wind speed distribution is fundamentally based on the used distribution functions. This paper examines five different distributions to describe the wind speed pattern, such as T Location-Scale, Logistic, Extreme Value, and Rayleigh distributions. Besides, alternative optimization algorithms like Multi-Verse Optimizer, Marine Predators Algorithm, and Grey Wolf Optimization are applied to the pre-described distributions to determine the best parameters. Five error measures are investigated and compared to test the accuracy of the presented distributions and optimization methods. Catalca site in Istanbul, Turkey, is chosen for this analysis. The analyzed results verify the applicability of the proposed approach to characterize the wind speed pattern. It was observed from the experimental results that the Rayleigh distribution occupied the highest rank, whereas the Extreme Value distribution was the worst. Many invaluable conclusions are also discussed based on the results and deep investigations.

1. Introduction

Modeling wind speed patterns and wind availability is crucial for multiple other essential studies. Modeling wind shape and potential primarily rely on wind speed patterns. Once the wind pattern is established, the wind availability can efficiently be specified. Therefore, wind shape characterization by different distributions is one of the most critical steps. Recently, numerous Probability Density Functions (PDFs) were introduced to describe wind speed profiles; among them, Rayleigh [3], Gamma [4], Weibull [1, 2], Lognormal [6], Normal [5], Logistical [7], Burr [10], Beta [8], Nakagami [9] distributions. Weibull, Rayleigh, and Gamma distributions [11-13] are the most commonly used distributions.

The Weibull distribution was used to investigate the statistical characteristics of wind speed at Catalca in Turkey [12]. Graphical, Energy Pattern Factor (EPF), and approximation estimation methods are utilized to estimate Weibull parameters. The Weibull distribution was also utilized [13] to assess the wind speed in Pakistan. The parameters were modeled using Particle Swarm Optimization (PSO), Cuckoo Search Optimization (CSO), and Grey Wolf Optimization (GWO). Empirical Method of Justus (EMJ), EPF, Method of Modified Maximum Likelihood (MML), and Moments (MOM) as numerical estimation methods were utilized. Many estimation techniques, such as Method of Moment (MOM), Mean least-squares (LS), Standard Deviation (MSD), Power Density (PD), EPF, and Genetic Algorithm (GA), to describe the wind speed distribution represented by Wadi and Elmasry [14]. Different error measures were introduced to evaluate the Goodness-Of-

---

[*] Corresponding author: Mohammed Wadi, Electrical & Electronics Engineering Department, Istanbul Sabahattin Zaim University, Istanbul, Turkey, E-mail: mohammed.wadi@izu.edu.tr
[1,2] Electrical & Electronics Engineering Department, Istanbul Sabahattin Zaim University, Istanbul, Turkey

Fitness (GOF) techniques used. The obtained outcomes demonstrated that GA outperformed all other methods, whereas the EPF occupied the lowest rank.

The EPF, empirical, graphical, and MML numerical estimation methods

to evaluate Weibull parameters, then to assess the capacity factor of wind turbines studied in [15]. MML method performed the most competent fitting, whereas the graphical method provided the worst. The wind speed at the airport site in Dolny Hricov based on Weibull, Gamma, and Lognormal was modeled [16]. Only the ML numerical estimation method was used to determine the optimal parameters. The Weibull with three-parameter occupied the first rank, whereas the Weibull with two-parameter was the second.

In some cases, due to the computations' complicated distribution parameters. Many distributions fail to describe the wind pattern due to its variability in other cases. Therefore, many researchers suggested alternative distributions [17, 18], like Birnbaum Saunders. The Birnbaum Saunders distribution to assess the wind pattern at ten locations in Ontario, Canada, is studied by Mohammadi et al. [18]. The analysed results showed that the Birnbaum Saunders distribution performance and matching outperformed the others.

Burr [10] and inverse Burr distributions [19-21] also have appeared in many research works. Wind data in Antakya, Turkey, were analysed by Burr distribution [10]. The results provided that the GOF of the Burr distribution matched more than others. [20] introduced the bi-parameter inverse Burr distribution used to assess the extreme wind speed values. Different estimation techniques like moment, ML, and quantile were utilized, and the results showed that the inverse Burr performed the best fitting.

Alternative distributions are needed to be applied; due to the variability of wind speed patterns from one location to another. Based on this role, this paper suggests an extensive examination to study the performance of alternative five distributions such as one-parameter Rayleigh, two-parameter Gamma, Extreme Value, and Logistic, and three-parameter T Location-Scale. Three optimization algorithms, Multi-Verse Optimizer (MVO), Grey Wolf Optimization (GWO), and Marine Predators Algorithm (MPA), are employed to evaluate the most acceptable parameters per distribution. Five error measures, net fitness, Mean Absolute Error (MAE), Correlation Coefficient (R), Regression Coefficient (R^2), and Root Mean Square Error (RMSE) are utilized to analyse and test these methods. Two years of wind data from the Catalca site is employed to conduct the analysis.

This paper is divided into sections: Section two explores the statistical PDFs, Cumulative Density Functions (CDFs), and Inverse CDFs (ICDFs) and their formulas per distribution. Section three introduces the process of determining the best parameters based on optimization algorithms. Section four explains the degree of accuracy per distribution based on different error measures. Besides, Section five illustrates the outcomes. Ultimately, Section six concludes the paper.

2. Statistical Distributions

As aforesaid, accurate modelling of the wind speed pattern is vital to assess wind energy potential in a particular area. Once the wind speed distribution pattern is accurately determined, the other features and analyses belonging to the location can be appropriately specified. Five different distributions were studied to model the distributions of wind speed data. After this, a concise explanation of these distributions is given.

2.1 Rayleigh Distribution

British physicist Lord Rayleigh initially derived Rayleigh distribution (RD). The one-parameter RD is a special case from the Weibull distribution when the shape parameter (k_W) equals two [22]. Due to its simplicity and the ability to accurately describe wind regimes, many research papers based on Rayleigh distribution to estimate the potential of wind at various locations worldwide were introduced [11, 23, 24]. Rayleigh PDF is defined as follows [25].

$$f(v) = \frac{2v}{b_R^2} \exp\left(-\frac{v}{b_R}\right)^2 \tag{1}$$

where $f(v)$ is the probability of observing wind speed v, $v = 0, 1, 2, \ldots, N$, N is the size of wind speed vector, and $b_R > 0$. The Rayleigh CDF, $F(v)$ and ICDF, $G(p)$ are defined according to equation (2) and equation (3), respectively.

$$F(v) = 1 - \exp\left(\frac{v^2}{2b_R^2}\right) \tag{2}$$

$$G(p) = b_R\sqrt{-2\ln(p-1)} \tag{3}$$

where $0 \leq p \leq 1$

2.2 Gamma Distribution

Gamma distribution (GD) is also a widely used distribution related mainly to Exponential and Normal distributions. Besides, many distributions such as Chi-squared, Exponential, and Erlang are special cases of the Gamma distribution. The Gamma PDF is expressed as:

$$f(v) = \frac{c_G^{k_G} v^{k_G-1} \exp(-c_G v)}{\Gamma(k_G)} \tag{4}$$

where k_G and $c_G > 0$, and Γ is the gamma function which has the following formula.

$$\Gamma(k_G) = \int_0^\infty t^{k_G-1} \exp(-t)\, dt \tag{5}$$

The Gamma distribution formulas for the CDF and ICDF are according to equations (6) and (8), respectively.

$$F(v) = \frac{\Gamma_v(\gamma)}{\Gamma(\gamma)}, v \geq 0; \gamma > 0 \tag{6}$$

where $\Gamma_v(\gamma)$ can be computed using the following equation.

$$\Gamma_v(k_G) = \int_0^v t^{k_G - 1} \exp(-t) dt \tag{7}$$

$$G(p) = \frac{1}{c_G^{k_G} \Gamma(k_G)} \int_0^v t^{k_G - 1} \exp\left(\frac{-t}{c_G}\right) dt \tag{8}$$

2.3 Extreme Value Distribution

Extreme Value distribution (EVD) has three identical types: type I (also called Gumbel distribution), type II (also known as Frechetandand), and type III (also called Weibull distributions). Every type has two representations, one depends on the minimum extreme and the other on the maximum extreme [26]. The general PDF formula of the two-parameter EVD of type I for both representations is defined as follows [27]:

$$f(v) = c_E^{-1} \exp\left(\frac{v - \lambda_E}{c_E}\right) \exp\left(-\exp\left(\frac{v - \lambda_E}{c_E}\right)\right) \tag{9}$$

where λ_E is the location parameter and c_E is the scale parameters.

One of the essential features of EVD its ability to model events with rare probability such as the highly-speed wind data [28, 29]. The CDF of EVD of type I for minimum and maximum extremes can be defined by the following Equations [29].

$$F(v) = 1 - \exp\left(-\exp\left(\frac{v - \lambda_E}{c_E}\right)\right), -\infty < v < \infty, c_E > 0 \tag{10}$$

$$F(v) = \exp(-\exp(-v)) \tag{11}$$

The ICDF of EVD of type I, also called percent point function, for minimum and maximum extremes are defined as in Equations (12) and (13), respectively [30].

$$G(p) = \ln\left(\ln\left(\frac{1}{1-p}\right)\right) \tag{12}$$

$$G(p) = -\ln\left(\ln\left(\frac{1}{p}\right)\right) \tag{13}$$

2.4 Logistic Distribution

Logistic distribution (LD), also referred to hyperbolic secant function distribution, is a continuous distribution [31]. It is similar to the Normal distribution in form with bigger tails. The PDF formula of LD is defined by the following Equation [32]:

$$f(v) = \frac{1}{4c_L} sech^2 \left(\frac{v - \mu_L}{2c_L} \right) \tag{14}$$

where μ_L and c_L are the mean and scale parameters.

The CDF of LD, which is also a scaled version of hyperbolic tangent distribution, has many applications in machine learning models such as logistic regression and feedforward neural networks. Its CDF can be computed using Equation (15) [33].

$$F(v) = 0.5 + 0.5 \tanh \left(\frac{v - \mu_L}{2c_L} \right) \tag{15}$$

The ICDF of LD can be defined as follows:

$$G(p) = \mu_L + c_L \ln \left(\frac{p}{1 - p} \right) \tag{16}$$

2.5 T Location-Scale Distribution

T Location-Scale distribution (TLSD) is a member of Location-Scale distributions family that based on three parameters, namely, location, scale, and shape. The PDF of TLSD can be given as follows [34]:

$$f(v) = \frac{\Gamma \left(\frac{k_T + 1}{2} \right)}{c_T \sqrt{k_T \pi} \, \Gamma \left(\frac{k_T}{2} \right)} \left[\frac{k_T + \left(\frac{v - \lambda_T}{c_T} \right)^2}{k_T} \right]^{-\frac{k_T + 1}{2}} \tag{17}$$

where $\Gamma(k_T)$ is the Gamma function that computes by Equation (18).

$$\Gamma(k_T) = \int_0^\infty t^{k_T - 1} \exp(-t) \, dt \tag{18}$$

One of the important features of TLSD is its property to represent the wind regimes with heavy tailed distributions [34]. It is worth to say, there is no closed formula for both CDF and ICDF of the three-parameter T Location-Scale distribution, but they can be calculated using iterative methods.

Table 1 summarizes all the used distributions along with the name and notation of their parameters.

Table 1: Parameters per distributions

Distributions	Number, (Name) of	Parameters

	parameters	
Rayleigh Distribution (RD)	1, (Defining parameter)	P1=b_R
Gamma Distribution (GD)	2, (Shape, Scale)	P1= k_G, P2= c_G
Extreme Value Distribution (EVD)	2, (Location, Scale)	P1= λ_E, P2= c_E
Logistic Distribution (LD)	2, (Mean, Scale)	P1=μ_L, P2=c_L
T Location-Scale Distribution (TLSD)	3, (Location, Scale, Shape)	P1= λ_T, P2=c_T, P3= k_T

3. Methodology

Evolutionary Optimization Algorithms (EOAs) utilize the mechanisms inspired by nature and solve problems via methods that imitate the behaviors of living organisms. EOAs represent a crucial pillar for solving nonlinear problems due to simplicity, flexibility, and ability to avoid local optima. However, they have drawbacks like computational complexity, convergence problems, and parameter initialization [35]. This section illustrates GWO, MPA, and MVO EOAs with their formulas, procedures, and flowcharts. The primary task of these algorithms is to find the best parameters per distribution.

3.1 Grey Wolf Optimization

The GWO algorithm simulates grey wolves hunting in nature. The hunting mechanism contains three stages, seeking a target, encircling the target, and attacking the target [36]. All search agents (grey wolves) in the collection (population) are initiated in a random way within the period [LB, UB], where LB and UB are the lower and upper borders of the parameters, respectively. Later, the fitness score per search agent is assessed by employing the objective function. The fitness solution is considered alpha along with beta and delta, respectively. Meantime, the rest of the grey wolves are organized under the omega. Therefore, in the GWO algorithm, the alpha, beta, and delta are computed, then the omega is found. Continuously, grey wolves update their locations depending on the target location as follows.

$$D_\alpha = |C_1 X_\alpha - X(t)|, D_\beta = |C_2 X_\beta - X(t)|, D_\delta = |C_3 X_\delta - X(t)| \qquad (19)$$

$$X_\alpha = X_\alpha - A_1 D_\alpha, X_\beta = X_\beta - A_2 D_\beta, X_\delta = X_\delta - A_3 D_\delta \qquad (20)$$

$$X(t+1) = \frac{X_\alpha + X_\beta + X_\delta}{3} \qquad (21)$$

where t and $t+1$ point to the current and the subsequent iterations sequentially. $X(t)$ and $X(t+1)$ are the current and following positions of the prey. X_α, X_β, and X_δ are the positions of alpha, beta, and delta, respectively. A and C are the coefficient vectors computed as follows:

$$A = 2a * r_1 - a \qquad (22)$$

374

$$C = 2r_2 \qquad\qquad (23)$$

where r_1 and r_2 are uniformly distributed random vectors within [0, 1], and a is the control vector that linearly decreased from 2 to 0. GWO repeats again from the step of the fitness evaluation and continues in the same procedure till the maximum iteration number is attained. Figure 1(a) shows the flowchart of GWO.
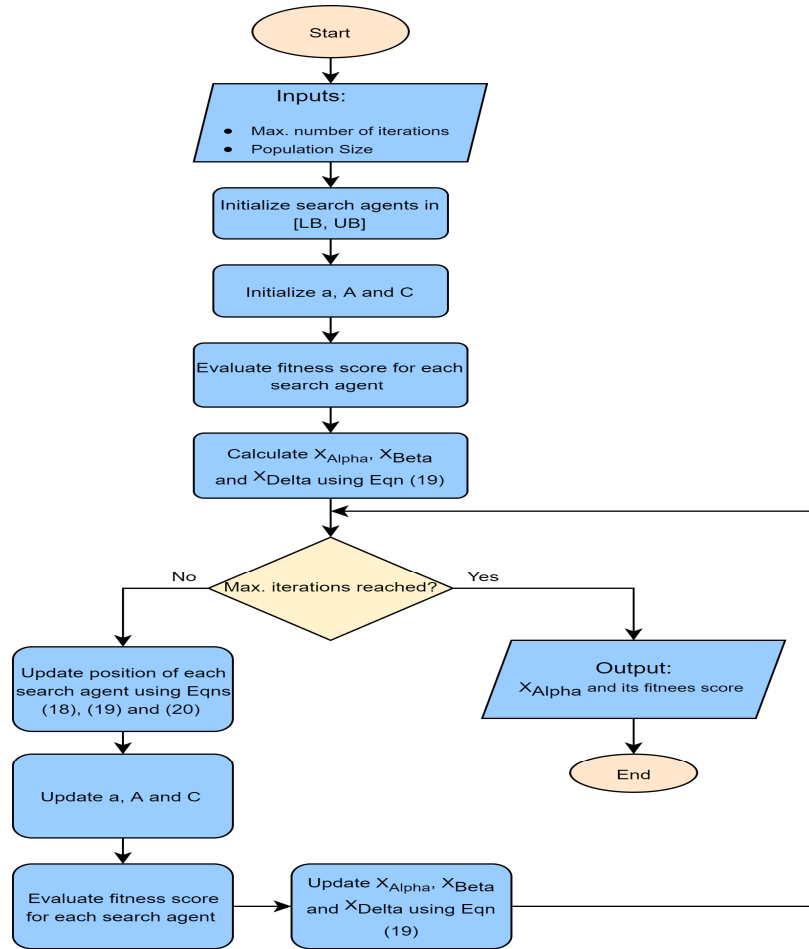

Figure 1: (a) Flowchart of GWO

3.2 Marine Predators Algorithm

MPA simulates the food foraging mechanism of marine predators [37]. Principally, marine predators rely on Levy and Brownian motion and the effects of vortex generation or Fish Aggregating Devices (FADs) [38] when searching for a target in seas. The MPA algorithm contains man stages. Initially, all search agents (marine predators) in the target matrix (population) are initiated randomly within the range [LB, UB]. The target matrix size is *NxM*, where *N* represents population size, and *M* represents the dimension of the problem variables, respectively. Later, the fitness score per search agent is assessed by the objective function. Then, the top predator is found. The optimal predator vector is repeated

375

many times to create the Elite matrix. The MPA first stage occurs when the target is moving quicker than the predator in which the most suited objective for the predator is to stay stable. This stage occurs in the first iteration, where the exploration process matters. Mathematically, *Iter* is the current iteration, and *Max − Iter* is the maximum iteration number; if *Iter < (1/3) Max_Iter*, predators adjust their locations in the target matrix as follows.

$$Stepsize_i = R_B \otimes \left(Elite_i - R_B \otimes Prey_i \right), i = 1, 2, ..., N \qquad (24)$$

$$Prey_i = Prey_i + P.R \otimes Stepsize_i \qquad (25)$$

where R_B, $\otimes$, P, R are vectors to generate random numbers using the normal distribution to simulate the Brownian movement, a notation preforms element-wise multiplications, a constant number equals 0.5, and a vector of random number uniformly distributed in [0, 1], respectively.

The second stage occurs when the predator and target move at about the same speed. This stage occurs when the exploration process starts to transform into exploitation. The predator is responsible for exploration, while the prey is for exploitation. Consequently, the predator drives in Brownian while the prey drives in Levy motion. Mathematically, when *(1/3) Max_Iter < Iter <(2/3) Max_Iter* , predators in the first half of Prey matrix change their positions using the following equations.

$$Stepsize_i = R_L \otimes \left(Elite_i - R_L \otimes Prey_i \right), i = 1, 2, ..., N \qquad (26)$$

$$Prey_i = Prey_i + P.R \otimes Stepsize_i \qquad (27)$$

where R_L is a vector of random numbers generated by Levy distribution. Meanwhile, in the second half of the Prey matrix, predators change their position as follows

$$Stepsize_i = R_B \otimes \left(R_B \otimes Elite_i - Prey_i \right), i = 1, 2, ..., N \qquad (28)$$

$$Prey_i = Elite_i + P.CF \otimes Stepsize_i \qquad (29)$$

$$CF = \left(1 - \frac{Iter}{Max\_Iter} \right)^{\left(2 \frac{Iter}{Max\_Iter} \right)} \qquad (30)$$

The third stage occurs when the predator moves faster than the target. This stage occurs when only the exploitation process matters. Therefore, the most helpful maneuvering for a predator is the Levy motion. Mathematically, when *Iter > (2/3) Max_Iter*, predators in the Prey matrix change their positions based on the following equations.

$$Stepsize_i = R_L \otimes \left(R_L \otimes Elite_i - Prey_i \right), i = 1, 2, ..., N \qquad (31)$$

$$Prey_i = Elite_i + P.CF \otimes Stepsize_i \qquad (32)$$

Then, MPA applies the effects of the eddy formations and *FADs* environments, as follows.

$$Prey_i = \begin{cases} Prey_i + CF \left[LB + R \otimes (UB - LB) \right] \otimes U & if\ r \le FADs \\ Prey_i + \left[FADs(1-r) + r \right] \left(Prey_{r1} - Prey_{r2} \right) & if\ r > FADs \end{cases} \qquad (33)$$

where *FADs* is a constant equals 0.2, U is a binary vector randomly distributed in [0, 1], and its array is changed to zero if it is less than 0.2 or to one; otherwise, r is a uniformly distributed random number within [0, 1], and r_1, r_2 indicate random indices in Prey matrix. Finally, MPA repeats again from the step of the fitness evaluation and continues in the same procedure until the maximum iteration numbers are satisfied. MPA outputs the top predator found so far and its fitness score. Figure 1 (b) depicts the flowchart of MPA.
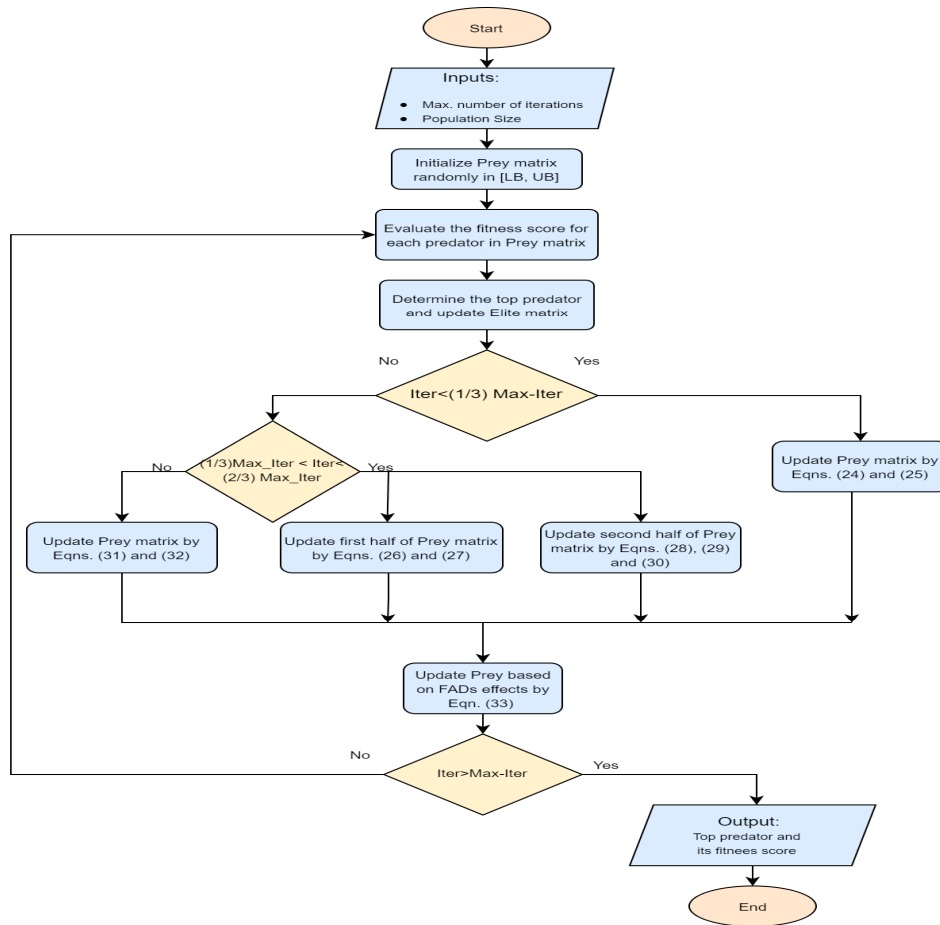

Figure 1: (b) Flowchart of MPA

3.3 Multi-Verse Optimizer

MVO simulates three cosmology concepts: white holes, black holes, and wormholes. The white or black holes and wormholes are designed to conduct exploration and exploitation operations in space. The MVO includes three phases: in the first phase, all search agents (universes) in the U matrix (population) are initiated randomly within the period [LB, UB]. The U matrix size is NxM, where N indicates the population size and M indicates the problem variables, respectively. Later, each search agent's fitness score (inflation rate) is assessed by the objective function. Then, the U matrix is sorted in the descending hierarchy. The most acceptable solution is renewed if the fitness score of the first universe in the sorted U is more reasonable than the fitness score of the current solution. Afterward, MVO permits moving objects from one universe with a higher inflation rate to another with a lower one. Therefore, the universe with a high inflation rate represents a white hole, whereas the universe with a nominal inflation rate denotes a black hole. Accordingly, an underpass between the two universes will be created to trade objects from white to black holes. Mathematically, to model white or black hole underpasses and the motion of objects through them, a roulette wheel is employed to choose one of the universes from the sorted U matrix. The white hole represents the specified universe by the roulette wheel. Each universe variable in U is renewed as follows.

$$x_i^j = \begin{cases} x_k^j & r_1 < NI(U_i) \\ x_i^j & r_1 \geq NI(U_i) \end{cases} \tag{35}$$

where x_i^j, x_k^j, r_1, and $NI(U_i)$ are the jth variable of the ith universe, the jth variable of the kth universe, a random number in [0, 1], and a normalized inflation rate of the ith universe, respectively.

Then, MVO allows the movement of objects randomly among universes (regardless their inflation rates) by using the concept of wormholes. Every universe in U matrix has a wormhole to transport the variables of the best solution explored so far to its variables randomly. Mathematically, for each universe in U matrix, its variables are updated using the following equation.

$$x_i^j = \begin{cases} X_j + TDR\left((UB_j - LB_j)r_4 + LB_j\right) & if\ r_3 < 0.5\ and\ r_2 < WEP \\ X_j - TDR\left((UB_j - LB_j)r_4 + LB_j\right) & if\ r_3 \geq 0.5\ and\ r_2 < WEP \\ x_i^j & if\ r_2 \geq WEP \end{cases} \tag{36}$$

where x_i^j is the jth variable of the ith universe, X_j is the jth variable of the best solution explored, *TDR* is the Travelling Distance Rate constant, *WEP* is a wormhole

existence probability constant, UB_j is the upper bound of the jth variable, LB_j is the lower bound of the jth variable, and r_2 to r_4 are random numbers within [0, 1].

Then, WEP and TDR constants are recalculated according to Equations (36) and (37), respectively.

$$WEP = min + l\left(\frac{max - min}{L}\right) \qquad (37)$$

where $min = 0.2$ and $max = 1$ are the minimum and maximum values of *WEP*, l is the current iteration, and L is the maximum iteration numbers.

$$TDR = 1 - \frac{l^{\frac{1}{p}}}{L^{\frac{1}{p}}} \qquad (38)$$

where p is the iterations exploitation accuracy and equals 6, finally, MVO repeats from the step of the fitness evaluation and continues in the same procedure until the maximum iteration number is fulfilled. MVO outputs the best solution explored so far and its fitness score. Figure 1(c) depicts the flowchart of MVO.
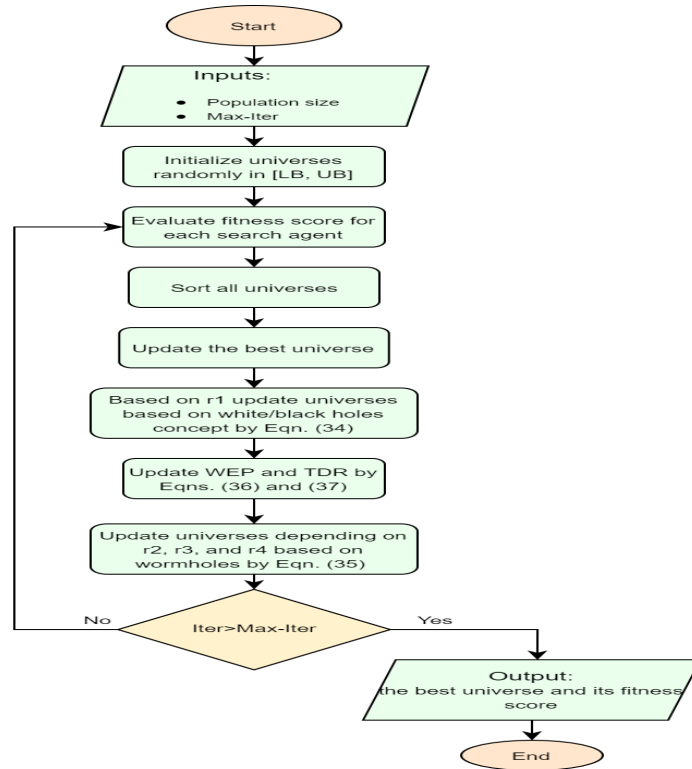

Figure 1: (c) Flowchart of MVO

3.4 Methodology

The distribution parameter selection is defined as a nonlinear optimization problem that minimizes the mean absolute error between the actual and expected wind speed vectors, as given below.

$$\min\left\{MAE\left(V_m, V_d\right)\right\} \tag{38}$$

where V_m and V_d are actual and expected wind speed vectors, respectively, V_d can be created by the ICDF of the distribution, as illustrated in Section 2.

To compute Equation (38), EOAs can find the best solution [39-42]. The search agents in GWO, MPA, and MVO algorithms, represent the candidate solutions to the problem. The selection of parameters per distribution represented by the search agent consists of integer values. The initial search agents population is created randomly within the [LB, UB] period. The fitness score per search agent is evaluated by Equation (38). Then, the population grows by exploring the highest solution based on the EOAs mechanism. The process continues until the number of maximum iterations is reached. Table 2 demonstrates the EOAs operation parameters.

Table 2: GWO, MPA and MVO operating values

Name of parameter	Range	Parameter Value
Population size	[5, 50]	50
Number of maximum iterations	[50, 300]	RD →100, GD→200, EVD, LD, and TLSD →300
Termination criteria	[1xE^{-4}, 1xE^{-6}]	1xE^{-6}

Table 3 illustrates the best parameter values per distribution based on the utilized three EOAs. In most cases, GWO, MPA, and MVO have almost the same parameter values. Regarding the running time, Table 4 shows the elapsed time of GWO, MPA, and MVO in seconds. It can be perceived that GWO is faster than others in convergence regarding all used distributions.

Table 3: Created parameters per distribution based on GWO, MPA and MVO algorithms

Distributions	Parameters	Datasets					
		2019			2020		
		GWO	MPA	MVO	GWO	MPA	MVO
RD	1st	3.25	3.25	3.24	3.46	3.46	3.46
GD	1st	3.33	3.34	3.33	2.86	2.87	2.65
	2nd	1.23	1.23	1.24	1.51	1.51	1.63
EVD	1st	4.81	4.81	4.76	5.03	5.03	4.95
	2nd	1.89	1.88	1.89	2.15	2.15	2.10
LD	1st	3.87	3.87	3.84	4.02	4.02	4.13

	2nd	1.42	1.42	1.39	1.58	1.58	1.61
TLSD	1st	3.85	3.85	3.93	4.03	4.01	4.03
	2nd	2.37	2.28	2.32	2.72	2.64	2.64
	3rd	345.39	8.37	14.15	614.77	24.25	33.54

4. Accuracy Measures

This paper employs numerous statistical measures to find the distribution and optimization algorithm with the most acceptable GOF. A brief with the formulas of each measure is given below:

Table 4: Elapsed running time of distributions in seconds

Distributions	Datasets					
	2019			2020		
	GWO	MPA	MVO	GWO	MPA	MVO
RD	3.71	7.80	4.47	4.66	9.26	13.57
GD	190.12	543.45	282.94	271.66	775.41	503.75
EVD	5.22	10.43	14.23	7.40	15.81	17.25
LD	10.51	21.03	26.16	12.59	26.23	31.53
TLSD	349.50	481.78	476.32	567.24	748.06	808.80

- *MAE* is the mean between the actual (x) and the expected (y) wind speed vectors as in Equation (39) [43].

$$MAE = \frac{\sum_{i=1}^{N} |y_i - x_i|}{N} \qquad (39)$$

where N is the length of wind speed vector.

- *RMSE* is the square root of the average of the differences between the expected and actual wind speeds [44]. It is computed by:

$$RMSE = \sqrt{\frac{\sum_{i=1}^{N} (y_i - x_i)^2}{N}} \qquad (40)$$

- *Regression Coefficient* defines the linearity grade between the expected wind speeds of distribution and the actual data. It computed by Equation (41).

$$R^2 = \frac{\sum_{i=1}^{N} (x_i - z_i)^2 - \sum_{i=1}^{N} (x_i - y_i)^2}{\sum_{i=1}^{N} (x_i - z_i)^2} \qquad (41)$$

381

where z_i is the ith actual mean wind speed.

- *Correlation Coefficient* demonstrates the correlation degree between the two datasets. It is defined within the period [-1, 1]. It can be computed as follows [45].

$$R = \frac{1}{N-1} \sum_{i=1}^{N} \frac{(x_i - \overline{x})(y_i - \overline{y})}{\sigma_x \sigma_y} \qquad (42)$$

where ($\overline{x}$, $\overline{y}$) and (σ_x , σ_y) indicates the mean and the standard deviation of the actual and the expected wind speed vectors, respectively.

- *Net Fitness* estimates the average of all the measures employed before. Again, the primary objective of using such a measure is to rank the used distributions based on their overall matching. It can be computed as follows [46].

$$Net\,Fitness = \frac{\sum_{i=1}^{n} |MAE_i| + \sum_{i=1}^{n} |RMSE_i| + \sum_{i=1}^{n} (1 - R_i^2) + \sum_{i=1}^{n} (1 - R_i)}{4n} \qquad (43)$$

where n is the total number of applied measures.

5. Results and Discussion

The collected data from the Catalca site in Turkey every 30 minutes at 10 m height for two years have been used to investigate the efficiency and the performance of the employed distributions and the optimization methods. Table 5 shows the details of the analyzed location.

Table 5: The Catalca location information

Station name	State	Country	Latitude (O) N	Longitude (O) E	Altitude (m)	Datasets
Ataturk	Istanbul	Turkey	40.967	28.817	37	2019 - 2020

Table 6: 2019-dataset average power and statistical calculations

EOA	Distributions	$\overline{x}$	σ	σ^2	Min	Max	Skew.	Kurt.	Average Power (W/m²)
-	Real	4.31	2.25	5.08	0.00	14.44	0.76	0.51	94.41
GWO	RD	4.32	2.12	4.51	0.37	13.95	0.62	0.28	88.95
	GD	4.37	2.28	5.21	0.59	18.02	1.10	1.82	100.79
	EVD	4.04	2.19	4.78	-4.72	8.99	-0.96	1.44	69.64
	LD	4.20	2.46	6.05	-3.28	16.92	0.22	1.04	93.96
	TLSD	4.15	2.29	5.26	-2.10	12.77	0.07	0.00	84.36
MPA	RD	4.32	2.12	4.51	0.37	13.95	0.62	0.28	88.93
	GD	4.37	2.28	5.21	0.59	18.02	1.10	1.82	100.77
	EVD	4.04	2.18	4.74	-4.69	8.98	-0.96	1.44	69.61
	LD	4.19	2.47	6.08	-3.30	16.94	0.22	1.04	94.00
	TLSD	4.18	2.50	6.23	-3.34	18.10	0.23	1.08	94.61

	RD	4.30	2.11	4.47	0.37	13.89	0.62	0.28	87.75
	GD	4.37	2.29	5.23	0.59	18.05	1.10	1.82	101.12
MVO	EVD	3.99	2.19	4.80	-4.79	8.96	-0.96	1.44	68.00
	LD	4.16	2.42	5.83	-3.18	16.65	0.22	1.04	90.69
	TLSD	4.25	2.40	5.76	-2.67	15.43	0.14	0.49	92.96

The illustrated EOAs, GWO, MPA, and MVO, are employed to assess the parameters per distribution. The utilized seven statistical descriptors, such as mean ($\overline{x}$), standard deviation (σ), variance (σ^2), minimum (Min), maximum (Max), skewness (Skew), kurtosis (Kurt), and average power, to define the pattern of the actual collected wind data. Tables 6 and 7 show the statistical analysis for the two datasets. The mean wind speed values at 10 m height for the 2019 and 2020 datasets of the actual data are about 4.30 and 4.50 m/s, respectively.

The wind speed mean value is a vital indication of wind potential at a specific location. Locations with high annual wind speed values are suitable for large-scale wind farms. The standard deviation value narrowly rises with an increase in the tower height. Variance is the square value of the standard deviation, measuring the divergence between wind speed values from their mean value. Also, variance narrowly rises with an increase in the tower height. The minimum actual wind speed is zero, while the maximum is 21.50 m/s.

The skewness measures the asymmetry from the dataset's average value. The obtained skewness values demonstrate that the actual data track the skewness of the positive distribution. Kurtosis whereas indicates the peaked grade of a distribution. Kurtosis has three classes; positive, negative, and zero [47]. The actual data tend to the kurtosis of positive shape.

The average power densities at the location at 10 m height are 94.40 and 111.70 W/m2 for the 2019 and 2020 datasets. It can be noticed that the average power density rises with an increase in the tower height [48-51]. Tables 6 and 7 show that the Rayleigh distribution accomplished the most acceptable matching, while the Extreme Value distribution delivered the worst.

Table 7: 2020-dataset average power and statistical calculations

EOA	Distributions	$\overline{x}$	σ	σ^2	Min	Max	Skew.	Kurt.	Average Power (W/m^2)
-	Real	4.5	2.5	6.2	0.0	15.6	0.6	0.2	111.7
GWO	RD	4.6	2.3	5.2	0.6	14.9	0.6	0.2	106.6
	GD	4.6	2.6	6.8	0.7	20.6	1.2	2.0	129.6
	EVD	4.1	2.5	6.2	-3.9	9.8	-0.8	0.8	82.1
	LD	4.4	2.7	7.5	-2.6	18.6	0.3	0.8	114.1
	TLSD	4.3	2.6	7.0	-1.9	14.2	0.1	-0.1	106.9
MPA	RD	4.6	2.3	5.2	0.6	14.9	0.6	0.2	106.6
	GD	4.6	2.6	6.8	0.7	20.6	1.2	2.0	129.5
	EVD	4.1	2.5	6.2	-3.9	9.8	-0.8	0.8	82.1
	LD	4.3	2.7	7.5	-2.5	18.6	0.3	0.8	114.0

	TLSD	4.3	2.7	7.1	-2.1	15.6	0.1	0.1	107.3
MVO	RD	4.6	2.3	5.2	0.6	14.9	0.6	0.2	106.8
	GD	4.6	2.7	7.3	0.6	21.5	1.2	2.2	135.1
	EVD	4.1	2.4	5.9	-3.8	9.6	-0.8	0.8	77.6
	LD	4.5	2.8	7.9	-2.6	19.0	0.3	0.8	123.0
	TLSD	4.3	2.6	6.9	-1.9	15.1	0.1	0.0	106.8

The distribution accomplishes the highest fitness when the difference between the actual and the expected data approaches zero. Tables 8 and 9 summarize the GOF of the presented distributions and EOAs. The values in bold indicate the most acceptable ones, whereas underlined values indicate the most acceptable at all. In most cases, Rayleigh distribution reached the best GOF. Conversely, Extreme Value distribution was the worst. In some cases, Gamma distribution delivered the most suitable matching in terms of MAE measure.

Table 8: 2019-dataset accuracy measures

EOA	Distributions	Accuracy measures				Net Fitness	Rank
		MAE	RMSE	R^2	R		
GWO	RD	0.141	**0.179**	**0.994**	**0.998**	0.082	1
	GD	**0.124**	0.210	0.991	0.996	0.087	2
	EVD	0.569	0.948	0.823	0.917	0.444	5
	LD	0.234	0.498	0.951	0.983	0.199	4
	TLSD	0.251	0.446	0.961	0.983	0.188	3
MPA	RD	0.141	**0.179**	**0.994**	**0.998**	0.082	1
	GD	**0.124**	0.210	0.991	0.996	0.087	2
	EVD	0.569	0.946	0.824	0.917	0.444	5
	LD	0.234	0.501	0.951	0.983	0.201	3
	TLSD	0.234	0.518	0.947	0.983	0.205	4
MVO	RD	0.144	**0.186**	**0.993**	**0.998**	0.085	1
	GD	**0.124**	0.212	0.991	0.996	0.087	2
	EVD	0.573	0.963	0.818	0.917	0.450	5
	LD	0.244	0.486	0.953	0.983	0.199	4
	TLSD	0.252	0.446	0.961	0.984	0.188	3

To firmly specify the accuracy of the best distribution, one average criterion called the net fitness test is required. Distributions are arranged according to four GOF tests. The rankings are established by considering a maximum of R^2 and R while a minimum of MAE and RMSE. Based on net fitness, the top-down rank of the five distributions based on both GWO, MPA, and MVO is Rayleigh, Gamma, T Location-Scale, Logistic, and Extreme Value. Table 10 shows the ranking of the five distributions. In addition, comparing Gamma and T location-scale distributions based on net fitness, it can be observed that there is a slight difference between them. On the other hand, based on computation time, T Location-

Scale distribution is more complex. For this site, Rayleigh distribution achieves the best in terms of matching and computation complexity.

Table 9: 2020-dataset accuracy measures

EOA	Distributions	Accuracy measures				Net Fitness	Rank
		MAE	RMSE	R^2	R		
GWO	RD	0.223	**0.271**	**0.988**	**0.9988**	0.127	1
	GD	**0.221**	0.381	0.977	0.9910	0.159	2
	EVD	0.594	0.978	0.846	0.9325	0.448	5
	LD	0.260	0.505	0.959	0.9871	0.205	4
	TLSD	0.233	0.433	0.969	0.9885	0.177	3
MPA	RD	0.223	**0.271**	**0.988**	**0.9988**	0.127	1
	GD	**0.221**	0.380	0.977	0.9911	0.158	2
	EVD	0.594	0.978	0.846	0.9325	0.449	5
	LD	0.260	0.504	0.959	0.9871	0.205	4
	TLSD	0.229	0.444	0.968	0.9889	0.179	3
MVO	RD	**0.223**	**0.271**	**0.988**	**0.9988**	0.127	1
	GD	0.228	0.441	0.969	0.9898	0.178	3
	EVD	0.609	0.995	0.841	0.9325	0.458	5
	LD	0.300	0.527	0.955	0.9871	0.221	4
	TLSD	0.231	0.426	0.971	0.9888	0.174	2

To display the obtained results visually for all datasets, Figures 2 and 3 depict the fitted PDFs and CDFs, respectively. In the PDF and CDF plots, the horizontal axis represents the wind speed in m/s. Regarding PDF plots, two different-scale vertical axes are used; the left one is for the histogram of the measured wind data, whereas the right is for the introduced distributions. These vertical axes represent the probability density. The vertical axis for CDF plots represents the cumulative density. Obviously, it is noticed from Figures 2 and 3 that all the introduced distributions achieved good matching. Rayleigh distribution occupied the first rank in terms of matching and computation complexity.

Table 10: Ranking of distributions using GWO, MPA and MVO

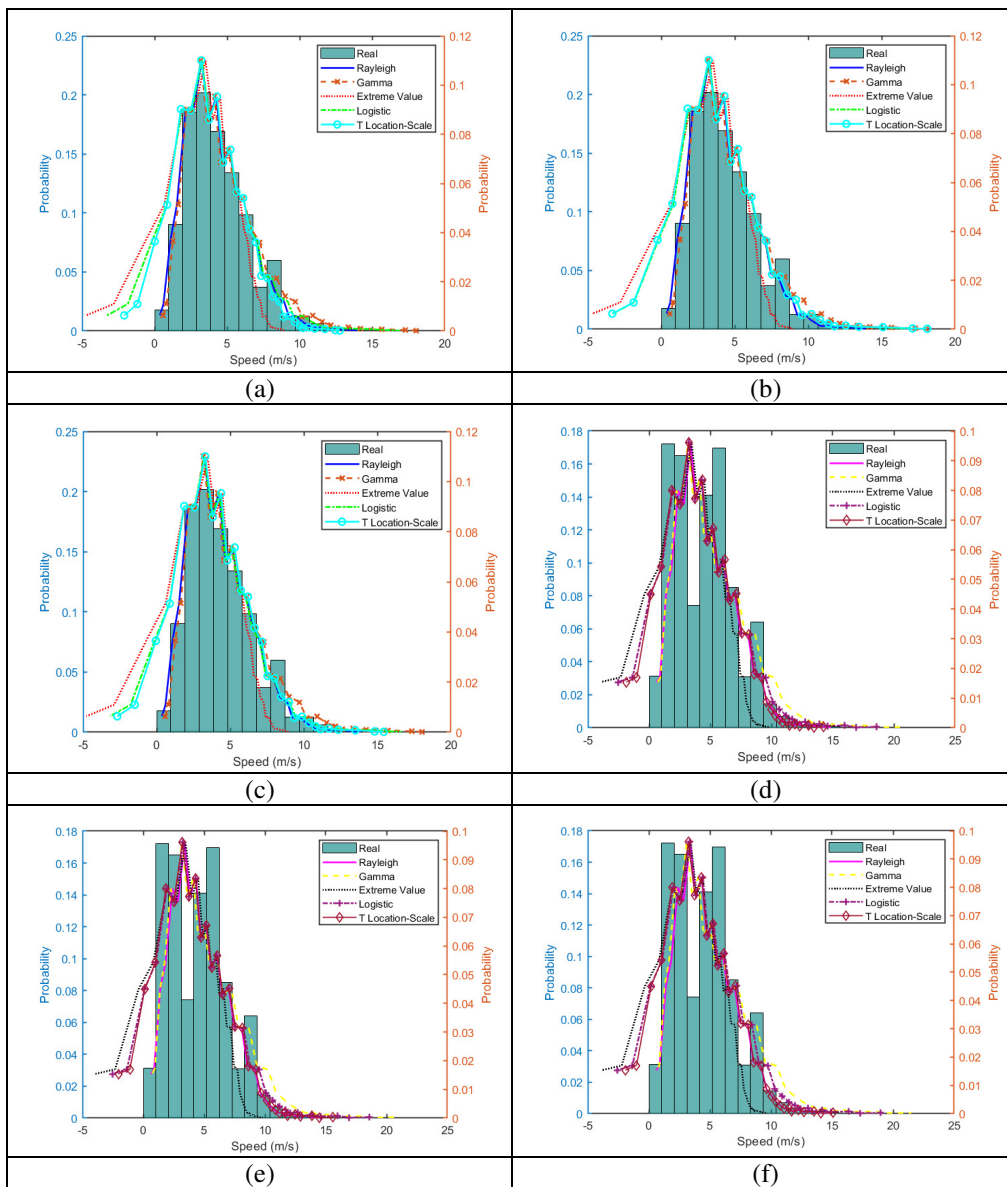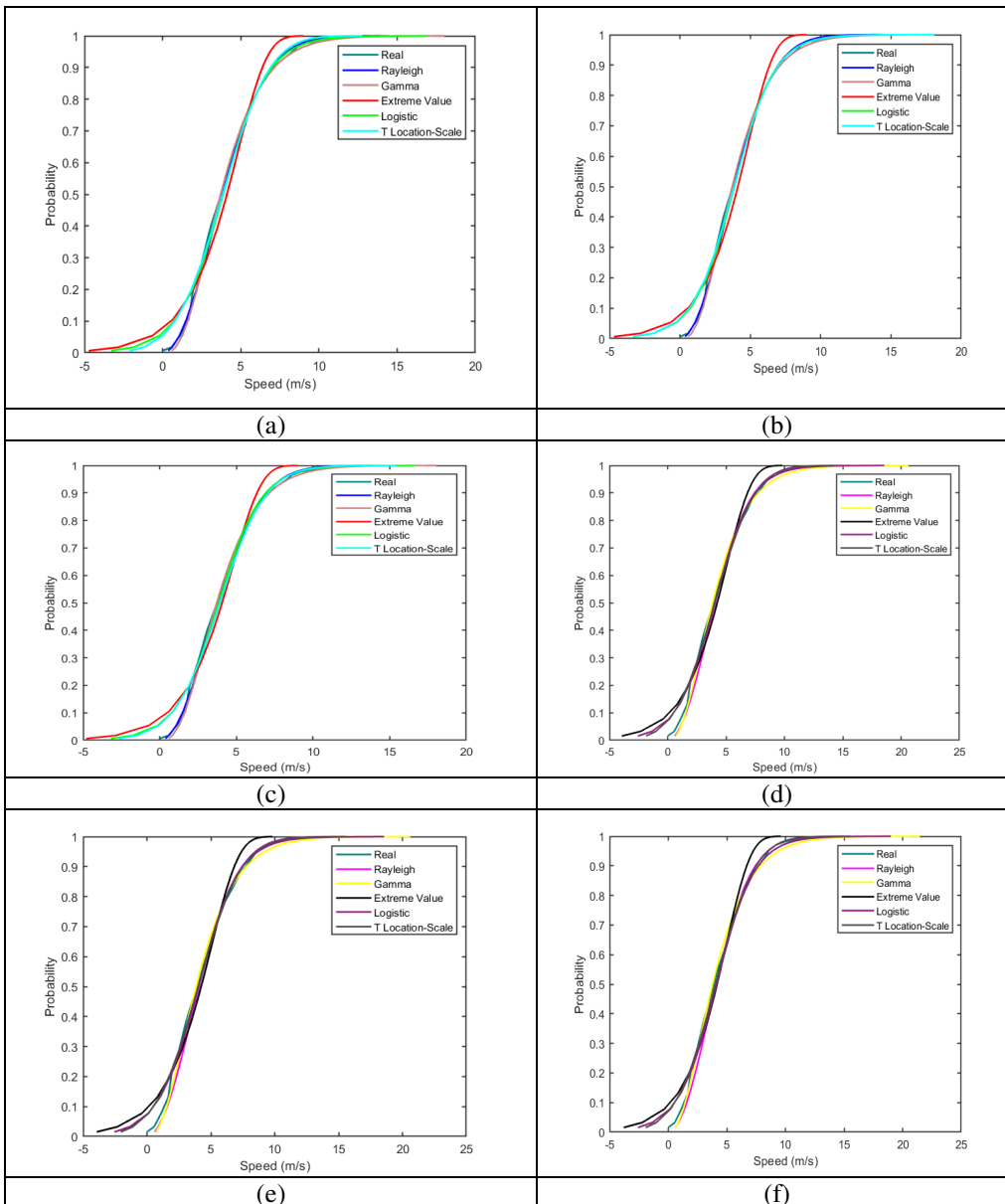| Distributions	2019					2020				
	1st	2nd	3rd	4th	5th	1st	2nd	3rd	4th	5th
RD	3	-	-	-	-	3	-	-	-	-
GD	-	3	-	-	-	-	2	1	-	-
EVD	-	-	-	-	3	-	-	-	-	3
LD	-	-	1	2	-	-	-	-	3	-
TLSD	-	-	2	1	-	-	1	2	-	-
Best	RD	GD	TLSD	LD	EVD	RD	GD	TLSD	LD	EVD

Figure 2: The PDF curves of introduced distributions when using: (a) GWO-2019, (b) MPA-2019, (c) MVO-2019, (d) GWO-2020, (e) MPA-2020, and (f) MVO-2020

Many invaluable deductions can be drawn from this study as follows:
- One of the most paramount deductions is related to the wind regime pattern that varies from one location to another and from year to year; therefore, various distributions should be utilized to describe the wind pattern accurately. In other words, a specific distribution function can accomplish the fittest GOF at a specific location but not at another.

Figure 3: The CDF curves of introduced distributions when using: (a) GWO-2019, (b) MPA-2019, (c) MVO-2019, (d) GWO-2020, (e) MPA-2020, and (f) MVO-2020

- The second important deduction is the selection of the optimization method. The success of the optimization method mainly depends on the features of wind speed data, computation complexity, and convergence. Consequently, the trade-off between various optimization methods is an indispensable requisite.
- The third important deduction is the applied error criteria. For example, a particular error measure may achieve the best with a particular distribution but the worst with another.

Consequently, it is crucial to use several error criteria. Afterward, to decide the rank of the estimation method accurately, the net fitness calculation is needed.

- The fourth significant deduction is the skewness and kurtosis statistical descriptor values which can also be crucial to describe the wind regime since they can display the whole wind distribution pattern. In this study, skewness and kurtosis values are positive. Therefore, the wind pattern takes the shape of positive skewness and leptokurtic. Accordingly, the selection of the convenient distribution can be recognized.

6. Conclusion

Many distribution functions are suggested to describe wind speed. However, alternative distributions are required due to the inability of some distributions and the computation complexities of others. This paper presents five alternative distributions to model the wind speed for two refresh data (2019&2020) at Catalca in Turkey. Three optimization algorithms, such as GWO, MPA, and MVO, are employed to determine the optimal parameter values per distribution. Many errors and statistical measures are utilized to specify the distribution and optimization with the best matching. The Rayleigh distribution outperformed the other distributions regarding computation complexity and best fitness. Conversely, the Extreme Value distribution provided the poorest matching. This study concludes with many essential findings to select the suitable distribution and optimization method that accurately helps describe the wind pattern at any site.

Author Contributions
All authors are involved in developing the concept to make the article error-free technical outcome for the set investigation work.

Conflicts of Interest
The authors declare that there are no conflicts of interest regarding the publication of this paper.

References

[1]   S. P. Komleh, A. Keyhani, and P. Sefeedpari, "Wind speed and power density analysis based on Weibull and Rayleigh distributions (a case study: Firouzkooh county of Iran)," *Renewable and Sustainable Energy Reviews*, vol. 42, pp. 313–322, 2015.
[2]   E. C. Morgan, M. Lackner, R. M. Vogel, and L. G. Baise, "Probability distributions for offshore wind speeds, "*Energy Conversion and Management*, Vol. 52, no. 1, pp. 15–26, 2011.
[3]   M. Wadi and W. Elmasry, "Modeling of wind energy potential in Marmara region using different statistical distributions and genetic algorithms," *International Conference on Electric Power Engineering–Palestine (ICEPE-P). IEEE*, 2021, pp. 1–7.
[4]   T. P. Chang, "Estimation of wind energy potential using different probability density functions, "*Applied Energy*, vol. 88, no. 5, pp. 1848–1856, 2011.
[5]   A. Garcia, J. Torres, and A. De Francisco, "Fitting wind speed distributions: a case study", Solar *energy*, vol. 62, no. 2, pp. 139–144, 1998.
[6]   H. L. Crutcher and L. Baer, "Computations from elliptical wind distribution statistics," *Journal of Applied Meteorology*, vol. 1, no. 4, pp. 522–530, 1962.

[7]   E. Scerri and R. Farrugia, "Wind data evaluation in the Maltese islands, "*Renewable energy*, vol. 7, no. 1, pp. 109–114, 1996.

[8]   I. Mert and C. Karakus, "A statistical analysis of wind speed data using burr, generalized gamma, and Weibull distributions in Antakya, Turkey, "*Turkish Journal of Electrical Engineering & Computer Sciences*, vol. 23, no. 6, pp. 1571–1586, 2015.

[9]   V. Yilmaz and H. E. Celik, "A statistical approach to estimate the wind speed distribution: the case of Gelibolu region," *Dogus Universitesi Dergisi*, vol. 9, no. 1, pp. 122–132, 2011.

[10]   O. Alavi, K. Mohammadi, and A. Mostafaeipour, "Evaluating the suitability of wind speed probability distribution models: A case of study of east and southeast parts of Iran," *Energy Conversion and Management*, vol. 119, pp. 101–108, 2016.

[11]   V. Sohoni, S. Gupta, and R. Nema, "A comparative analysis of wind speed probability distributions for wind power assessment of four sites, "*Turkish Journal of Electrical Engineering & Computer Sciences*, vol. 24, no. 6, pp. 4724–4735, 2016.

[12]   M. Wadi, B. Kekezoglu, M. Baysal, M. R. Tur, and A. Shobole, "Feasibility study of wind energy potential in Turkey: Case study of catalca district inistanbul," in2019 2nd International Conference on Smart Grid and Renewable Energy (SGRE). IEEE, 2019, pp. 1–6.

[13]   M. Gul, N. Tai, W. Huang, M. H. Nadeem, and M. Yu, "Evaluation of wind energy potential using an optimum approach based on maximum distance metric," *Sustainability*, vol. 12, no. 5, p. 1999, 2020.

[14]   M. Wadi and W. Elmasry, "Statistical analysis of wind energy potential using different estimation methods for Weibull parameters: a case study, "*Electrical Engineering*, pp. 1–22, 2021.

[15]   B. K. Saxena and K. V. S. Rao, "Comparison of Weibull parameters computation methods and analytical estimation of wind turbine capacity factor using polynomial power curve model: case study of a wind farm, "*Renewables: Wind, Water, and Solar*, vol. 2, no. 1, p. 3, 2015.

[16]   I. Pobocıkov ́a, Z. Sedliackova, and M. Michalkova, "Application of four probability distributions for wind speed modeling," *Procedia engineering*, vol.192, pp. 713–718, 2017.

[17]   V. Leiva, M. Barros, G. A. Paula, and M. Galea, "Influence diagnostics in log-Birnbaum–Saunders regression models with censored data, "*Computational Statistics & Data Analysis*, vol. 51, no. 12, pp. 5694–5707, 2007.

[18]   K. Mohammadi, O. Alavi, and J. G. McGowan, "Use of Birnbaum Saunders distribution for estimating wind speed and wind power probability distributions: A review, "*Energy Conversion and Management*, vol. 143, pp. 109–122, 2017.

[19]   E. Chiodo, "The burr xii model and its bayes estimation for wind power production assessment, "*International Review of Electrical Engineering (IREE)*, vol. 8, no. 2, pp. 737–751, 2013.

[20]   E. Chiodo and P. De Falco, "Inverse burr distribution for extreme wind speed prediction: Genesis, identification and estimation, "*Electric Power Systems Research*, vol. 141, pp. 549–561, 2016.

[21]   B. KOSE, M. DUZ, M. T. GUNES¸ER, and Z. Recebli, "Estimating wind energy potential with predicting burr LSM parameters: A different approach. "*Sigma: Journal of Engineering & Natural Sciences/Muhendislik ve Fen Bilimleri Dergisi*, vol. 36, no. 2, 2018.

[22]   B. Hoxha, R. Selimaj, and S. Osmanaj, "An experimental study of Weibull and Rayleigh distribution functions of wind speeds in Kosovo,"*TELKOMNIKA(Telecommunication, Computing, Electronics and Control)*, vol. 16, no. 5, pp. 2451–2457, 2018.

[23]   Y. Arikan, O. P. Arslan, and E. Cam, "The analysis of wind data with Rayleigh distribution and optimum turbine and cost analysis in Elmadag, Turkey, "*Istanbul University - Journal of Electrical and Electronics Engineering*, 2015.

[24]   H. Bidaoui, I. El Abbassi, A. El Bouardi, and A. Darcherif, "Wind speed data analysis using Weibull and Rayleigh distribution functions, case study: fivecities northern morocco," *Procedia Manufacturing*, vol. 32, pp. 786–793, 2019.

[25]   F. Maleki Jebely, K. Zare, and E. Deiri, "Efficient estimation of the PDF and the CDF of the inverse Rayleigh distribution," *Journal of Statistical Computation and Simulation*, vol. 88, no. 1, pp. 75–88, 2018.

[26]   M. Rajabi and R. Modarres, "Extreme value frequency analysis of wind data from Isfahan, Iran," *Journal of wind Engineering and industrial Aerodynamics*, Vol. 96, no. 1, pp. 78–82, 2008.

[27]   Y. Quan, F. Wang, and M. Gu, "A method for estimation of extreme values of wind pressure on buildings based on the generalized extreme-value theory, "*Mathematical Problems in Engineering*, vol. 2014, 2014.

[28]   F. Van Der Heijden, R. P. Duin, D. De Ridder, and D. M. Tax, Classification, parameter estimation and state estimation: an engineering approach usingMATLAB. John Wiley & Sons, 2005.

[29]   Y. Xiao, Q. Li, Z. Li, Y. Chow, and G. Li, "Probability distributions of extreme wind speed and its occurrence interval, "*Engineering Structures*, vol. 28, no. 8, pp. 1173–1181, 2006.

[30]   B. Abolpour, B. Abolpour, H. Bakhshi, and M. Yaghobi, "An appropriate extreme value distribution for the annual extreme gust winds speed *Fundam Renewable Energy Appl*, vol. 7, no. 223, p. 2, 2017.

[31]   M. Freimer, G. Kollia, G. S. Mudholkar, and C. T. Lin, "A study of the generalized Tukey lambda family, "*Communications in Statistics-Theory and Methods*, vol. 17, no. 10, pp. 3547–3567, 1988.

[32]   W. Lin, J. Wen, S. Cheng, and W.-J. Lee, "An investigation on the active-power variations of wind farms," *IEEE Transactions on Industry Applications*, Vol. 48, no. 3, pp. 1087–1094, 2012.

389

[33] S. R. Bowling, M. T. Khasawneh, S. Kaewkuekool, and B. R. Cho, "A logistic approximation to the cumulative normal distribution, "*Journal of Industrial Engineering and Management*, vol. 2, no. 1, pp. 114–127, 2009.

[34] A. Morteza and M. Amirmazlaghani, "A novel statistical approach for multiplicative speckle removal using t-locations scale and non-sub sampled shearlet transform, "*Digital Signal Processing*, vol. 107, p. 102857, 2020.

[35] D. Guha, P. K. Roy, and S. Banerjee, "Load frequency control of large-scale power system using quasi-oppositional grey wolf optimization algorithm, "*Engineering Science and Technology, an International Journal*, vol. 19, no. 4, pp. 1693–1713, 2016.

[36] S. Mirjalili, S. M. Mirjalili, and A. Lewis, "Grey wolf optimizer, "*Advances in engineering software*, vol. 69, pp. 46–61, 2014.

[37] A. Faramarzi, M. Heidarinejad, S. Mirjalili, and A. H. Gandomi, "Marine predators algorithm: A nature-inspired metaheuristic," *Expert Systems with Applications*, vol. 152, p. 113377, 2020.

[38] N. E. Humphries, N. Queiroz, J. R. Dyer, N. G. Pade, M. K. Musyl, K. M. Schaefer, D. W. Fuller, J. M. Brunnschweiler, T. K. Doyle, J. D. Houghtonet al., "Environmental context explains levy and brownian movement patterns of marine predators, "*Nature*, vol. 465, no. 7301, pp. 1066–1069, 2010.

[39] J. D. Filmalter, L. Dagorn, P. D. Cowley, and M. Taquet, "First descriptions of the behaviour of silky sharks, Carcharhinus falciform is, around drifting fishaggregating devices in the indian ocean,"*Bulletin of Marine Science*, vol. 87, no. 3, pp. 325–337, 2011.

[40] S. Mirjalili, S. M. Mirjalili, and A. Hatamlou, "Multi-verse optimizer: a nature-inspired algorithm for global optimization, "*Neural Computing and Applications*, vol. 27, no. 2, pp. 495–513, 2016.

[41] W. Elmasry, M. Wadi, "Detection of Faults in Electrical Power Grids Using an Enhanced Anomaly-Based Method", *Arabian Journal for Science and Engineering*, 1-16, 2022.

[42] M. Wadi, W. Elmasry, A. Shobole, M. R. Tur, R. Bayindir, and H. Shahinzadeh, "Wind Energy Potential Approximation with Various Metaheuristic Optimization Techniques Deployment" *7th International Conference on Signal Processing and Intelligent Systems (ICSPIS)*, Tehran, Iran, pp. 1-6, 2021.

[43] M. Wadi, M. R. Tur, and M. Tanrioven, "Optimization of Distributed Generation Using Homer Software and Fuzzy Logic Control", *3rd European Conference on Renewable Energy Systems*, Antalya, Turkey, pp. 7-10, 2015.

[44] M. Wadi, M. Baysal, A. Shobole, and Tur, M. R., "Reliability evaluation in smart grids via modified Monte Carlo simulation method", *7th International Conference on Renewable Energy Research and Applications (ICRERA)*, Paris, France, pp. 841-845, 2018.

[45] A. Shobole, Wadi, M. "Multiagent systems application for the smart grid protection", *Renewable and Sustainable Energy Rev.*, vol. 149, 2021.

[46] C. J. Willmott and K. Matsuura, "Advantages of the mean absolute error (MAE) over the root mean square error (RMSE) in assessing average model performance, "*Climate research*, vol. 30, no. 1, pp. 79–82, 2005.

[47] R. J. Hyndman and A. B. Koehler, "Another look at measures of forecast accuracy, "*International journal of forecasting*, vol. 22, no. 4, pp. 679–688, 2006.

[48] A. Papoulis and S. U. Pillai, Probability, random variables, and stochastic processes. *Tata McGraw-Hill Education*, 2002.

[49] M. Gul, N. Tai, W. Huang, M. H. Nadeem, and M. Yu, "Evaluation of wind energy potential using an optimum approach based on maximum distance metric, "*Sustainability*, vol. 12, no. 5, p. 1999, 2020.

[50] L. T. DeCarlo, "On the meaning and use of kurtosis. *Psychological methods*, vol. 2, no. 3, p. 292, 1997.

[51] Wadi, M., "Fault detection in power grids based on improved supervised machine learning binary classification", *Journal of Electrical Engineering*, 72(5), 315-322, 2021.

[52] M. Wadi., "Five different distributions and metaheuristics to model wind speed distribution", *J Ther Eng*;7(8):1–23, 2021.

[53] M. Wadi, M. Baysal, and A. Shobole, "Reliability and Sensitivity Analysis for Closed-Ring Distribution Power Systems", *Electric Power Components and Systems*, 49(6-7), pp. 696-714, 2022.